Invited Paper

THz Generation Using Cherenkov Phase Matching

Kei Takeya [1*], Koji Suizu [2] and Kodo Kawase [1, 3]
[1] Nagoya University, Furo-cho, Chikusa-ku, Nagoya, Japan
[2] Chiba Institute of Technology, Tsudanuma, Narashino, Chiba, Japan
[3] RIKEN, Aramaki-aoba, Aoba-ku, Sendai, Japan
[*1] Email: takeya@nuee.nagoya-u.ac.jp

(Received June 25 2012)

Abstract: An efficient terahertz (THz) wave generation based on Cherenkov type radiation from non-linear optical (NLO) crystals is presented in this paper. In terms of the THz generation from NLO crystals, it is well known that the high absorptivity and the phase mismatch prevent the effective THz generation. Using Cherenkov type THz radiation, we solved the problems and obtained an advantage that many crystals can be used as THz wave emitters. The successful generation of monochromatic THz waves is demonstrated with wide tunability in the range 0.2–3.0 *THz*. We obtained the enhancement factor of about 50 as a result of a suppression of phase miss-matching with surfing configuration for bulk NLO crystal. In addition, using prism-coupled Cherenkov phase-matching (PCC-PM) method with the organic crystal 4-dimethylamino-N-metyl-4-stilbazolium tosylate (DAST), we achieved THz-wave radiation with wide-tunability with no deep absorption features. The obtained spectra did not depend on the pump wavelength.

Keywords: Cherenkov phase matching, $LiNbO_3$, Terahertz, prism-coupled Cherenkov phase-matching (PCC-PM)

doi: 10.11906/TST.078-086.2012.06.07

1. Introduction

Recent development of terahertz (THz) technology is remarkable in many fields. The improvement of THz devices is essential to the development of THz science and technology [1-2]. The development of monochromatic and tunable coherent THz sources is of great importance for use in these applications. Recently, a parametric process based on second-order nonlinearities was used to generate tunable, monochromatic, coherent THz sources using nonlinear optical (NLO) crystals such as 4-dimethylamino-N-metyl-4-stilbazolium tosylate (DAST), $LiNbO_3$, $LiTaO_3$, GaAs and so on [3-7]. Further, various researchers reported the studies based on difference frequency generation (DFG) [8-11], optical rectification [12-13] or coherent phonon emission [14-16]. In terms of the effective THz generation, the high absorption coefficient of NLO crystals prevents the effective THz generation. Since the refractive index of NLO crystals is different between the optical and THz frequencies, phase matching condition and coherent length of optical rectification process are also issues for effective THz radiation. To overcome these issues for progress, our group has reported the methods based on surface emitting or waveguide propagation with Cherenkov-type radiation using NLO crystals [17-22]. This method shows following advantages; absorption is minimized because the THz wave is generated at the crystal surface: the phase matching condition is relaxed using a suitable cladding material. In this paper, we present an efficient THz wave generation from surface emitting and waveguide propagation using Cherenkov type radiation with NLO crystals.

The Cherenkov phase-matching condition is satisfied when the velocity of the polarization

wave inside the nonlinear crystal is greater than that of the radiated wave outside. The radiation angle θ is determined by the refractive index of the pumping wave in the crystal, n_{opt}, and that of THz-wave in the crystal, n_{THz} [23],

$$\cos\theta = \frac{\lambda_{THz}/n_{THz}}{2Lc} = \frac{\lambda_{THz}/n_{THz}}{\lambda_1\lambda_2/(n_1\lambda_2 - n_2\lambda_1)} \cong \frac{n_{opt}}{n_{THz}}, \quad (1)$$

where λ is a wavelength of the contributing waves in the DFG process ($\omega_1 - \omega_2 = \omega_{THz}$) and Lc is the coherence length of the surface-emitted process ($Lc = \pi/\Delta k$, where $\Delta k = k_1 - k_2$ and k is the wave number). We approximate the refractive index of the optical wave as $n_1 \approx n_2 = n_{opt}$ because λ_1 and λ_2 have almost the same value for THz-wave generation. Equation (1) implies that n_{THz} should be larger than n_{opt}. The lithium niobate crystal has a refractive index of about 2.1 in the near infrared region, and has a refractive index of about 5.1 in the THz-wave region. The generated THz-wave is totally reflected at the interface of air and the lithium niobate crystal. The silicon prevents total internal reflection of THz waves at the interface of air and the lithium niobate crystal.

The radiation angle hardly changes during THz-frequency tuning because the silicon has low refractive index dispersion in the THz-wave region [24] and the optical wavelength requires only slight tuning. The change in radiation angle is less than 0.01° for a fixed pumping wavelength. The actual angle change of the THz wave is significantly better than for the THz parametric oscillator (TPO) with a Si prism coupler [25], which has an angle change of about 1.5° in the 0.7–3 *THz* tuning range.

2. Monochromatic THz-wave generation based on Cherenkov phase-match

We demonstrated the method described above using the experimental setup shown in Figure 1. The frequency-doubled Nd:YAG laser, which has pulse duration of 15 *ns*, a pulse energy of 12 *mJ* when operating at 532 *nm*, and a repetition rate of 50 *Hz*, was used as the pump source for a dual-wavelength potassium titanium oxide phosphate (KTP) optical parametric oscillator (OPO). The KTP-OPO, which consists of two KTP crystals with independently controlled angles, is capable of dual-wavelength operation with independent tuning of each wavelength [26-27]. The OPO has a tunable range of 1300 to 1600 *nm*. The maximum output energy of 2 *mJ* was obtained for a pumping energy of less than 12 *mJ*. The 5 mol% MgO-doped lithium niobate crystal ($MgO:LiNbO_3$) used in the experiment was cut from a 5 × 65 × 6 *mm* wafer, and the *x*-surfaces at both ends were mirror-polished. An array of seven Si prism couplers was placed on the *y*-surface of the $MgO:LiNbO_3$ crystal. The *y*-surface was also mirror-polished to minimize the coupling gap between the prism base and the crystal surface, and to prevent scattering of the pump beam, which excites a free carrier at the Si prism base. To increase the power density, the pump beam diameter was reduced to 0.3 *mm*. The polarizations of the pump and THz waves were both parallel to the *z*-axis of the crystals. The THz-wave output was measured with a fixed 4 *K* Si bolometer.

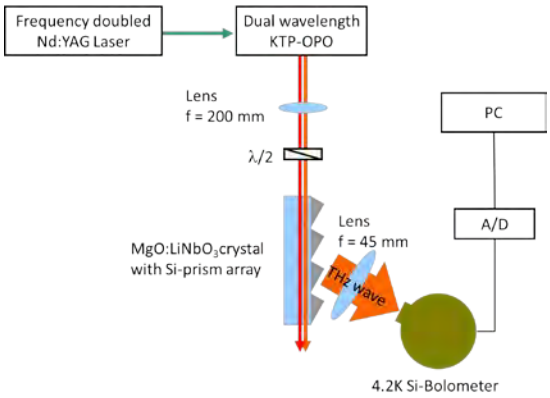

Fig. 1 Experimental setup for Cherenkov phase-matching monochromatic THz-wave generation.

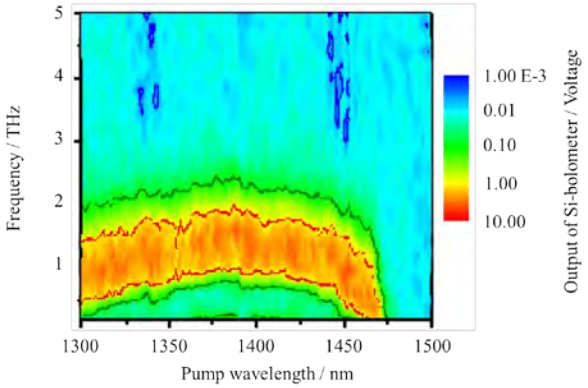

Fig. 2 THz-wave output mapping for various pump wavelengths and corresponding THz-wave frequencies. The *x*-axis and *y*-axis denote the pump wavelength, λ_1, and the THz-wave frequency, respectively. The magnitude of the map values indicates the output voltage of the detector. The blue, green, and red curves are contour plots corresponding to the detector output voltages of 10 *mV*, 100 *mV*, and 1 *V*, respectively.

The THz-wave output map for various pumping wavelengths and corresponding THz-wave frequencies is shown in Figure 2. The magnitude of the map denotes the output voltage of a Si bolometer with a gain of 200. The noise level of the bolometer was about 10 *mV* and is shown as the blue region in the figure. The regions where 100 *mV* and 1 *V* of output voltage were obtained are green and red, respectively. The blue, green, and red curves are contour plots for 10 *mV*, 100 *mV*, and 1 *V*, respectively. As seen in the figure, wide tunability in the range 0.2–3.0 *THz* was obtained by choosing the proper pumping wavelength. Especially for lower frequency below 1.0 *THz*, this was very efficient compared to our previous TPO systems that used 1470 *nm* pumping.

3. THz-wave generation from surface of bulk $LiNbO_3$ crystal

Here, we propose surfing configuration of Cherenkov type phase matching for THz wave generation for bulk crystal to suppress a phase mismatching. Interference pattern of pumping waves in the crystal is induced by combining the dual wavelengths beams with finite angle. It provides a same spatial pattern of second order nonlinear polarization in THz frequency. The interference pattern has not checkerboard one, which is a results of interference of tilted beams with same frequency, like as mentioned in Ref. [28], because dual wavelength beam courses

other spatial interference pattern, corresponding to difference frequency, and the interference pattern is superimposed in checkerboard one.

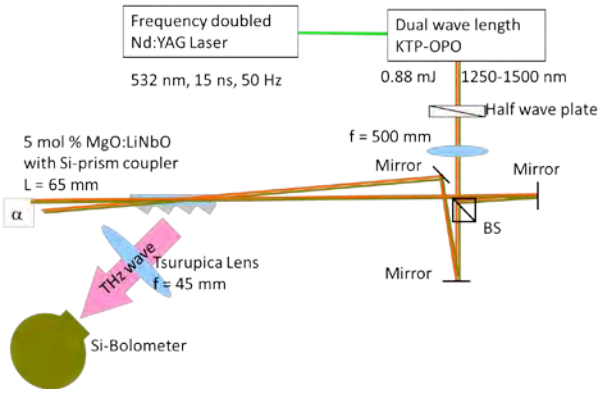

Fig. 3 Schematic of experimental setup for Cherenkov phase-matching THz-wave generation with surfing configuration.

Figure 3 shows the schematic of experimental setup. A pump source for DFG process was same as our previous works [26], which has a tunable range of 1250 to 1500 *nm*, 15 *ns* of pulse duration and 0.88 *mJ* of pulse energy. An output of the source with dual wavelength was focused by circular lens ($f = 500$ *mm*) before divided by half beam splitter, and combined again with finite angle. The spot diameter of the combined beam was 0.45 *mm*. The MgO:$LiNbO_3$ used in the experiment was cut from a $5 \times 65 \times 6$ *mm* wafer, and the *x*-surfaces at both ends were mirror-polished. An array of seven Si prism couplers was placed on the *y*-surface of the MgO:$LiNbO_3$ crystal. To minimize the coupling gap between the crystal surface and the prism base, the *y*-surface of LN was also mirror polished. This polished surface prevented scattering of the pump beam, which generates free carriers at the Si-prism base. The THz waves and polarizations of the pump were both parallel to the *z*-axis of the crystal. The THz-wave output was measured with a fixed 4-K Si bolometer.

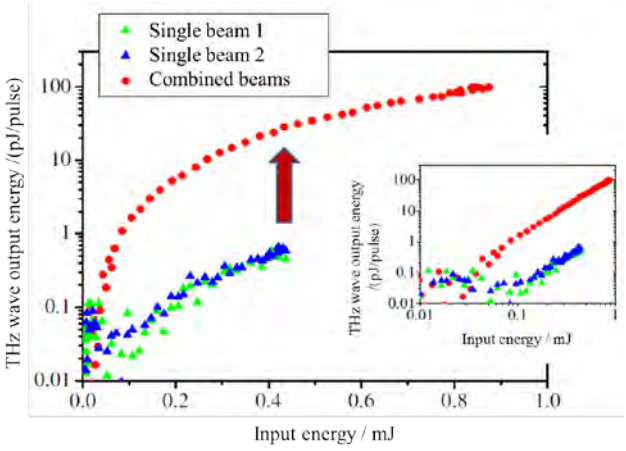

Fig. 4 Input-output properties of the THz-wave for 1.0 *THz* generation with $\alpha = 2.49°$. The circles and triangles denote the THz-wave output signal for the combined beams and single beams, respectively. The inset shows a double logarithmic plot of the input−output properties.

Input-output properties of THz-wave for pumping energy are shown in Figure 4 at 1.0 *THz* generation with $\alpha = 2.49$ *degrees*. Circles and triangles denotes THz-wave output signal with

combined beams and with single beam by dumping the other beam before entrance to the crystal, respectively. Maximum pumping energy of only 0.44 *mJ* was achieved at single beam pumping, because a half of whole pumping energy was dumped as shown in Figure 3. The vertical axis is the THz-wave pulse energy calculated from the output voltage of a Si-bolometer detector, a pulse energy of about 101 *pJ/pulse* corresponded to a Si-bolometer voltage output of 1 *V* when the repetition rate was less than 200 *Hz*. As shown in the figure, remarkable enhancement of THz-wave generation with surfing configuration, whose magnetic was about 50 *times*, was successfully observed. Inset of Figure 4 shows double logarithmic plot of input-output properties. Slope efficiency under combined beams and single beam pumping were almost same values. It means that enhancement factor of about 50 was a result of a suppression of phase miss-matching.

4. Prism-coupled Cherenkov phase-matched THz-wave generation using a DAST crystal

Cherenkov THz radiation is generated inside a nonlinear crystal when the velocity of the polarization excited by a DFG process is greater than the phase velocity of the radiated wave. In general, many nonlinear crystals have strong dispersion between the optical and THz regions, and the refractive index at THz frequencies is larger than that at optical frequencies. This may result in behavior that satisfies the equation (1). The Cherenkov angle, θ_{crystal}, is determined by the refractive index at the pump frequencies and that at the THz frequency in the crystal, and so the angle is strongly dependent on the nonlinear material. The emitted THz radiation propagates with the Cherenkov angle to the crystal–air interface, and if the angle is greater than a critical angle, which is determined by the difference in the refractive index at the interface, the THz wave undergoes total internal reflection at the interface. In order to prevent this, we use a cladding material with a suitable refractive index formed into a prism. The angle of the cladding–nonlinear crystal interface, θ_{clad}, is important for practical applications and can be determined using Snell's law, as follows.

$$\begin{aligned}\theta_{clad} &= \frac{\pi}{2} - \beta = \frac{\pi}{2} - \arcsin\left(\frac{n_{THz}}{n_{clad}}\sin(\alpha)\right) \\ &= \frac{\pi}{2} - \arcsin\left(\frac{n_{THz}}{n_{clad}}\sin\left(\frac{\pi}{2} - \theta_{crystal}\right)\right) \\ &= \frac{\pi}{2} - \arcsin\left(\frac{n_{THz}}{n_{clad}}\sin\left(\frac{\pi}{2} - \arccos\left(\frac{n_1\lambda_2 - n_2\lambda_1}{n_{THz}(\lambda_2 - \lambda_1)}\right)\right)\right) \\ &= \arccos\left(\frac{n_1\lambda_2 - n_2\lambda_1}{n_{clad}(\lambda_2 - \lambda_1)}\right)\end{aligned} \tag{2}$$

where n_{clad} is the refractive index of the cladding layer in the THz-frequency range. This equation is equivalent to a model in which the THz wave radiates directly into the cladding layer. It indicates that n_{clad} should be larger than that of the nonlinear crystal at the pump frequency, and also that it is not necessary to take into account the refractive index of the crystal at the THz frequency (as the equation does not depend on n_{THz}). We call the method as Prism Coupled Cherenkov Phase Matching (PCC-PM). For the PCC-PM THz-wave generation, by comparing the refractive index of the crystal at optical frequencies to that of Si (which is approximately 3.4 across the whole of the THz-frequency region), we see that Si is suitable as a Cherenkov

radiation output coupler for many nonlinear crystals.

Fortunately, Eq. (2) tells us that the Cherenkov condition inside the crystal does not have to be satisfied for THz generation using the PCC-PM method. The THz radiation experiences the refractive index of the cladding material at the interface, and so it can be coupled out from the cladding layer, regardless of the relative refractive indices within the nonlinear crystal, with an almost fixed angle. The calculated angles inside the crystal range from 0° to 40°, and the THz radiation is totally reflected at the interface with air, as predicted from Eq. (2). If the Si cladding functions only as an output coupler, it follows that the Si coupler will not work as a Cherenkov phase-matching component, and the THz radiation at the frequency where the phase matching condition is not satisfied cannot be out-coupled unless the Si cladding is formed into a prism.

We used a 100-*μm*-thick DAST single crystal in this experiment. The crystal was hexagonal, so that we could achieve *b*-axis propagation of two pump beams. A Si prism was coupled along the (001) plane of the DAST crystal because as-grown DAST has a very flat surface in the plane. A dual-wavelength KTP-OPO with pulse duration of 15 *ns*, pulse energy of 1.5 *mJ*, and 1300–1600-*nm* tunable range was used as a pump, as in our previous work. [17-20] The polarizations of the two pumps were parallel to the *a*-axis of the DAST crystal, which has the highest nonlinear coefficient component, and THz radiation was generated parallel to the *a*-axis. The pump beam was focused to form a 46-*μm* diameter beam using a cylindrical lens with a 50-*mm* focal length, resulting in a power density of about 50 *MW/cm*2. The emitted THz radiation was detected using a liquid-helium-cooled Si bolometer with an electrical gain of 1000.

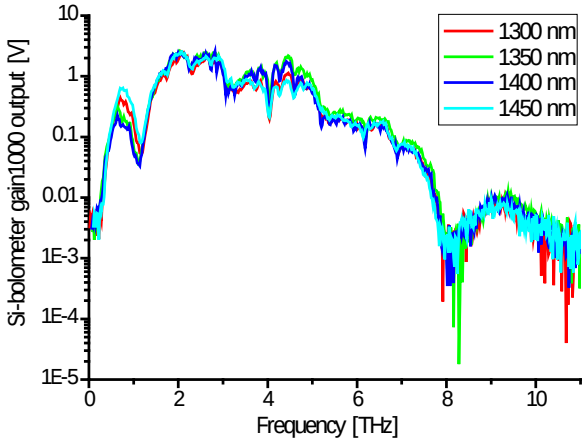

Fig. 5 THz output spectra under pump wavelengths ranging from 1300−1450 *nm*.

Figure 5 shows the collected THz output spectra under different pump wavelengths. THz radiation was generated at levels from less than 1 *THz* to more than 10 *THz*, with spectra that were almost independent of the pump wavelength. The dip at 8 *THz* was originated from the transmission character of a filter inside the Si-bolometer. When collinear phase matching is used to generate THz radiation, a deep dip in the spectra is observed at around 1.1 *THz*. [26, 29] This is suppressed here because the Cherenkov method results in surface emission, and we successfully obtained about 100 *times* higher signal compared to noise level of the detector. Additionally, radiation was generated below 1 *THz*, which cannot be generated using collinear phase matching with 1300–1450-*nm* pumping [30]. At frequencies above ~10 *THz*, the detection

efficiency of the bolometer falls off, and this explains the low observed power at higher frequencies. However, the collected power extends to higher frequencies than were observed when using bulk lithium niobate in our previous works [18]. Although THz radiation generated far from the crystal–cladding interface interferes with that generated near the interface, resulting in destructive interference, the radiation generated deep within the crystal is attenuated due to the large absorption coefficient of the crystal. The absorption coefficient of DAST crystal at around 2–10 *THz* is 100–200 cm^{-1}. The beam diameter was approximately 50 μm, and so the intensity of a THz-wave that propagates this distance will be attenuated by 30-60%. The output voltage of the Si bolometer can be converted to energy by considering that 1 $V \approx 20$ *pJ/pulse* for the low-repetition-rate detection and that we have a gain of 1000 at the bolometer. The highest-energy THz pulse obtained was about 50 *pJ* (3.3 *mW* at peak). The obtained output energy was higher than that of obtained by collinear phase matching condition using DAST crystal under almost same power density [26, 29].

We demonstrated the PCC-PM THz generation using a DAST crystal. The spectra were broadband and almost independent of the pump wavelength over a range 1300–1450 *nm*. The PCC-PM method has the advantage of suppressing the strong absorption due to the nonlinear crystal. The conversion efficiency using collinear and non-collinear phase matching methods is inversely proportional to square of the absorption coefficient, and the large nonlinearity in the crystal cannot be fully exploited due to the large absorbance. The great potential of organic nonlinear crystals can be effectively exploited using this method because surface emission is not influenced by absorption in the crystal. Hebling et al. described a figure of merit of several nonlinear crystals [31] from the viewpoint of the nonlinearity and absorption coefficient. GaSe had the highest figure of merit; however, DAST has a larger optical nonlinearity. Using the surface-emission method described here, the absorption coefficient ceases to be an issue, suggesting that DAST may be a more efficient material for generating THz radiation using DFG. The method described here has the advantage of relaxing the phase-matching condition. Many crystals require that a phase-matching condition (such as birefringence, non-collinear, and quasi phase matching) is satisfied, however, the PCC-PM method provides a much less stringent phase-matching condition. Furthermore, the method does not require a specific pump wavelength. This method could allow the realization of simple, compact, highly efficient, and ultra-broadband THz sources using a range of nonlinear crystals.

5. Conclusions

We reported THz wave generation based on the Cherenkov-type radiation using bulk crystal. In section 2, we presented a Cherenkov phase-matching method for monochromatic THz-wave generation using the DFG process with a $LiNbO_3$ crystal, which resulted in both high conversion efficiency and wide tunability. Section 3 presented Cherenkov phase matching with a “surfing” configuration for the bulk crystal. Efficient THz-wave generation and a high enhancement factor were obtained. In section 4, we presented the PCC-PM method, in which a prism with a suitable refractive index at THz frequencies was coupled to the crystal. Using a DAST crystal, this method produced THz-wave radiation with wide tunability; no deep absorption features were evident, and the obtained spectra did not depend on the pump wavelength.

ACKNOWLEDGMENT

The authors thank Dr. T. Shibuya, Dr. H. Minamide, and Prof. H. Ito of RIKEN for their experimental support for the part of the work.

References

[1] M. Tonouchi, "Cutting-edge terahertz technology", *Nat. Photon*. 1, 97-105, (2007).

[2] B. Ferguson. and X.-C. Zhang, "Materials for terahertz science and technology", *Nat. Mater.*, 1, 1, 26-33, (2002).

[3] J. M. Yarborough, S. S. Sussman, H. E. Purhoff, R. H. Pantell, and B. C. Johnson, "Efficient, tunable optical emission from $LiNbO_3$ without a resonator", *Appl. Phys. Lett*., 15, 5, 102–105, (1969).

[4] B. C. Johnson, H. E. Puthoff, J. SooHoo, and S. S. Sussman, "Power and linewidth of tunable stimulated far-infrared emission in $LiNbO_3$", *Appl. Phys. Lett.*, 18 5, 181–183, (1971).

[5] M. A. Piestrup, R. N. Fleming, and R. H. Pantell, "Continuously tunable submillimeter wave source"，*Appl. Phys. Lett*., 26, 8, 418–421, (1975).

[6] K. Kawase, M. Sato, T. Taniuchi, and H. Ito, "Coherent tunable THz-wave generation from $LiNbO_3$ with monolithic grating coupler", *Appl. Phys. Lett*., 68, 18, 2483–2485, (1996).

[7] K. Kawase, H. Minamide, K. Imai, J. Shikata, and H. Ito, "Injection-seeded terahertz-wave parametric generator with wide tenability", *Appl. Phys. Lett*., 80, 2, 195–197, (2002).

[8] G. D. Boyd, T. J. Bridges, C. K. N. Patel, and E. Buehler, "Phase matched submillimeter wave generation by difference-frequency mixing in ZnGeP2", *Appl. Phys. Lett*., 21, 11, 553–555, (1972).

[9] W. Shi, Y. J. Ding, N. Fernelius, and K. Vodopyanov, "Efficient, tunable, and coherent 0.18–5.27-THz source based on GaSe crystal", *Opt. Lett*., 27, 16, 1454–1456, (2002).

[10] T. Tanabe, K. Suto, J. Nishizawa, K. Saito, and T. Kimura, "Tunable terahertz wave generation in the 3- to 7-THz region from GaP", *Appl. Phys. Lett.*, 83, 237–239, (2003).

[11] K. Kawase, M. Mizuno, S. Sohma, H. Takahashi, T. Taniuchi, Y. Urata, S. Wada, H. Tashiro, and H. Ito, "Difference-frequency terahertz-wave generation from DAST by use of an electronically tuned Ti: sapphire laser", *Opt. Lett*. 24, 1065–1067, (1999).

[12] D. H. Auston, "Subpicosecond electro-optic shock waves", *Appl. Phys. Lett.*, 43, 713–715, (1983).

[13] L. Xu, X.‐C. Zhang, and D. H. Auston, "Terahertz beam generation by femtosecond optical pulses in electro‐optic materials", *Appl. Phys. Lett*., 61, 1784‐1786, (1992).

[14] K. H. Yang, P. L. Richards, and Y. R. Shen, "Coherent phonon generation by optical mixing in a one-dimensional superlattice", *J. Appl. Phys*. 44, 1417-1419, (1973).

[15] T. Dekorsy, H. Auer, C. Waschke, H. J. Bakker, H. G. Roskos, H. Kurz, V. Wagner, and P. Grosse , "Emission of Submillimeter Electromagnetic Waves by Coherent Phonons", *Phys. Rev. Lett*. 74, 738–741, (1995).

[16] K. Takeya, Y. Takemoto, I. Kawayama, H. Murakami, T. Matsukawa, M. Yoshimura, Y. Mori and M. Tonouchi, "Terahertz emission from coherent phonons in lithium ternary chalcopyrite crystals illuminated by 1560 nm femtosecond laser pulses", *EPL*. 91, 20004-1-4, (2010).

[17] K. Suizu, T. Shibuya, T. Akiba, T. Tutui, C. Otani, and K. Kawase, "Cherenkov phase-matched monochromatic THz-wave generation using difference frequency generation with lithium niobate crystal", *Opt. Exp*., 16, 7493–7498, (2008).

[18] T. Shibuya, T. Tsutsui, K. Suizu, T. Akiba, and K. Kawase, "Efficient cherenkov-type phase-matched widely tunable THz-wave generation via an optimized pump beam shape", *Appl. Phys. Exp*., 2, 032302-1-3, (2009)

[19] K. Suizu, K. Koketsu, T. Shibuya, T. Tsutsui, T. Akiba, and K. Kawase, "Extremely frequency-widened terahertz wave generation using Cherenkov-type radiation", *Opt. Exp*., 17, 6676–6681, (2009).

[20] K. Suizu, T. Tsutsui, T. Shibuya, T. Akiba, and K. Kawase, "Cherenkov phase-matched THz-wave generation with surfing configuration for bulk lithium niobate crystal", *Opt. Exp*., 17, 7102–7109, (2009).

[21] K. Suizu, T. Shibuya, H. Uchida, and K. Kawase, "Prism-coupled Cherenkov phase-matched terahertz wave generation using a DAST crystal", *Opt. Exp*., 18, 3338–3344, (2010).

[22] K. Kawase, S. Ichino, K. Suizu and T. Shibuya, "Half Cycle Terahertz Pulse Generation by Prism-Coupled Cherenkov Phase-Matching Method", *J. Infrared Milli. Terahz. Waves*, 32, 1168–1177, (2011).

[23] R. L. Sutherland, "Handbook of Nonlinear Optics", *Chap. 2. Marcel Dekker*, New York, (2003).

[24] D. Grischkowsky, S. Keiding, M. van Exter, and Ch. Fattinger, "Far-infrared time-domain spectroscopy with terahertz beams of dielectrics and semiconductors", *J. Opt. Soc. Am. B*, 7, 2006–2015, (1990).

[25] K. Kawase, J. Shikata, H. Minamide, K. Imai, and H. Ito, "Arrayed silicon prism coupler for a terahertz-wave parametric oscillator", *Appl. Opt*., 40, 9, 1423–1426, (2001).

[26] H. Ito, K. Suizu, T. Yamashita, T. Sato, and A. Nawahara, "Random frequency accessible broad tunable terahertz-wave source using phase-matched 4-dimethylamino-N-methyl-4-stilbazolium tosylate crystal", *Jpn. J. Appl. Phys*., 46, 11, 7321–7324, (2007).

[27] K. Suizu, T. Shibuya, S. Nagano, T. Akiba, K. Edamatsu, H. Ito, and K. Kawase, "Pulsed high peak power millimeter wave generation via difference frequency generation using periodically poled lithium niobate", *Jpn. J. Appl. Phys*., 46, 40, L982–L984, (2007).

[28] J. K. Wahlstrand and R. Merlin, "Cherenkov radiation emitted by ultrafast laser pulses and the generation of coherent polaritons", *Phys. Rev. B*, 68, 054301-1-12, (2003).

[29] K. Suizu, K. Miyamoto, T. Yamashita, and H. Ito, "High-power terahertz-wave generation using DAST crystal and detection using mid-infrared power-meter", *Opt. Lett*., 32, 2885–2887, (2007).

[30] T. Taniuchi, S. Ikeda, S. Okada, and H. Nakanishi, "Tunable Sub-Terahertz Wave Generation from an Organic DAST Crystal", *Jpn. J. Appl. Phys*., 44, L652–L654, (2005).

[31] J. Hebling, A. G. Stepanov, G. Almasi, B. Bartal, and J. Kuhl, "Tunable THz pulse generation by optical rectification of ultrashort laser pulses with tilted pulse fronts", *Appl. Phys. B*., 78, 593–599, (2004).